Published in final edited form as:
J Chem Theory Comput. 2012 February 14; 8(2): 749–758. doi:10.1021/ct200790q.

Modification of Lipid Bilayer Structure by Diacylglycerol: A Comparative Study of Diacylglycerol and Cholesterol

Mohammad Alwarawrah, **Jian Dai**, and **Juyang Huang***
Department of Physics Texas Tech University Lubbock, Texas 79409

Abstract

Diacylglycerols (DAGs) are important second messengers in biomembranes, and they can activate protein kinase C and many other enzymes and receptors. However, their interactions with cholesterol and other lipids have not been previously studied using molecular dynamics (MD) simulation. In this study, nine independent atomistic MD simulations were performed to specifically investigate the interactions between di16:0DAG, 16:0,18:1-phosphatidylcholine (POPC), and cholesterol. Despite of their substantial differences in chemical structure, DAG and cholesterol produce some very similar effects in POPC bilayers: increasing acyl chain order and bilayer thickness, reducing volume-per-lipid, and decreasing lateral diffusion of molecules. More significantly, DAG also produces a strong “condensing effect” in PC bilayers. In comparison, cholesterol is more effective than DAG in producing the above effects. The driving force for the condensing effect is their molecular shape: DAG and cholesterol both have small polar headgroups and large hydrophobic bodies. In a lipid bilayer, in order to avoid the unfavorable exposure of their hydrophobic parts to water, neighboring phospholipid headgroups move toward cholesterol or DAG to provide cover. Thus, seemingly complex interactions between DAG, cholesterol and phospholipid can be clearly explained using the Umbrella Model. Our simulations confirmed the hypothesis that DAG increases the spacing between phospholipid headgroups, which is important for activating protein kinase C and other enzymes. Interestingly, our simulations also show that the conventional wisdom that the spacing created by a DAG is directly above the DAG molecule is incorrect; instead, the largest spacing usually occurs between the first and the second nearest-neighbor PC headgroups from a DAG, due to the umbrella effect.

Keywords

Umbrella Model; diffusion coefficient; cholesterol-lipid interaction; order parameter; headgroup spacing

INTRODUCTION

Diacylglycerols (DAGs) play important roles in lipid metabolism and cell signaling, and are well known for activating protein kinase C and other enzymes and receptors.[1,2] DAG can be produced in cell membranes either as a result of the hydrolysis of phosphatidylinositol 4,5-bisphosphate (PIP2) or phosphatidylcholine. It has been shown that DAGs can modify the phospholipid bilayer structure significantly or even induce non-bilayer phases at high concentration.[3,4] As a molecule with a small headgroup and a large hydrophobic body, DAG

*Corresponding author: Juyang Huang, Department of Physics, Texas Tech University, Lubbock, Texas, 79409; Tel.: (806)742-4780; Fax: (806)742-1182; juyang.huang@ttu.edu.

SUPPORTING INFORMATION: dag_itp.doc is a GROMACS force field for di16:0DAG. This file is available free of charge via the Internet at http://pubs.acs.org.

increases the spacing between phospholipid headgroups in lipid bilayers. Using ^{2}H NMR and ESR techniques, Schorn and Marsh found that DAGs are incorporated into bilayer membranes similar to phospholipids incorporation, but are situated approximately two CH_2 groups deeper in the hydrophobic interior.[5]

In a fluid-phase lipid bilayer, cholesterol increases the order of acyl chains and bilayer thickness, and reduces the lateral diffusion of lipids. The most well known effect of cholesterol is the “cholesterol condensing effect”, i.e., the total area of a lipid bilayer becomes less than the sum of the areas of phospholipids and cholesterol.[6-8] Molecular dynamics (MD) simulation has become a powerful tool to investigate detailed interactions between molecules at the atomistic level. Although the interactions of cholesterol with phospholipids have been extensively studied in the past decade[9-17], DAG-cholesterol-phospholipid interactions have not yet been investigated using MD simulation. Recently, Pandit et al. showed that ceramide and cholesterol have a very similar effect on POPC bilayers, although ceramide is less effective in increasing chain order compared to cholesterol.[18] In this study, various effects of di16:0DAG on POPC bilayers with or without cholesterol have been investigated. By comparing the effects produced by cholesterol or by DAG, the molecular driving force of DAG-phospholipid interaction will be examined.

The chemical structures of di16:0DAG, cholesterol, and POPC are shown in Figure 1a. Despite their vast differences in structure, DAG and cholesterol produce some very similar effects on POPC bilayers: increasing acyl chain order and bilayer thickness, reducing area per lipid, and decreasing lateral diffusion. More significantly, we found that DAG also induces strong “condensing effect” in PC bilayers. However, cholesterol is more effective than DAG in producing such effects, probably due to its rigid sterol rings. We hypothesize that the similarity in their effects on PC bilayers is resulted from their similarity in molecular shape: DAG and cholesterol both have small hydrophilic headgroups and large hydrophobic bodies. In a lipid bilayer, cholesterol mainly relies on the coverage of neighboring phospholipid headgroups to avoid the unfavorable exposure of its hydrophobic part to water, as described by the Umbrella Model.[19,20] The cholesterol condensing effect is resulted from the tight packing between cholesterol and PC needed to achieve the coverage. The same mechanism also produces the condensing effect of DAG. Our result clearly explains the previous experimental finding that cholesterol can “amplify” DAG's activity.[21] An important consequence of the umbrella coverage is that the largest spacing created by a DAG in a lipid bilayer is not directly over the DAG molecule, as described in some papers; rather, we find it to be between the first and the second nearest-neighbor PC headgroups from a DAG.

In terms of cross-sectional area, DAG has a smaller headgroup/body ratio than cholesterol. Our 2D radial distribution functions of molecules show that DAGs receive more Umbrella coverage than cholesterol in POPC bilayers. Interestingly, we found that unlike cholesterol, DAG is not solely relying on the Umbrella coverage, it can also reduce the unfavorable exposure by inserting its acyl chains into surrounding chain matrix (i.e., lateral insertion), particularly at low DAG concentrations. Our electron density profiles show that DAG in the POPC/DAG bilayer is situated about 1.9 Å deeper into the bilayer interior than POPC, which agrees well with previous experimental results.[5]

SIMULATION METHODS

Nine independent simulations of pure, binary and ternary mixtures consisting of POPC, DAG, and cholesterol, were performed at 310 K with a time step of 2.0 fs. The first four systems in Table 1 were run for 500 ns, and the rest five were run for 300 ns. The total number of lipids in each system was kept at 512. The phospholipid force field was from

Berger et al.,[22] and the cholesterol force field was based on the GROMOS force field from Holtje et al.[23] Since DAG has not been previously studied using MD simulation, its force field must be created. DAG force field (see SUPPORTING INFORMATION) was constructed from the bonded and non-bonded parameters of GROMOS87 force field[24] implemented in GROMACS as ffgmx. The atomic charges for a DAG were obtained using QM calculations. The partial charges were calculated using ORCA package (http://www.thch.uni-bonn.de/tc/orca/) at hybrid functional B3LYP/G level as defined in Gaussian program system[25-28] with 6-31G* basis set[29-31]. All systems were run in the NPT ensemble using a Nosé-Hoover thermostat[32] and Parrinello-Rahman barostat[33] methods with a coupling time constant of 0.1 and 1.0 ps, respectively. The pressure normal and parallel to the bilayer were coupled separately at 1 bar. The LINCS algorithm was used to keep the lengths of all bonds constant. Long-range electrostatic interactions were handled with the particle mesh Ewald (PME) method.[34] The cutoff distances for Lennard-Jones interactions and electrostatic interactions were both set at 1.0 nm. All other simulation conditions were identical to that in our previous studies.[9,11]

Creating initial structures

The lipid bilayer was constructed by first obtaining the PDB coordinates file of a single POPC molecule from Dr. Peter Tieleman's Website, and the initial structure of di16:0DAG was constructed using the Dundee PRODRG2 Server[35]. A single POPC was placed inside a solvent box, and a short simulation was performed to relax the lipid. Afterward, bilayers of 32, 64 and 512 POPCs were constructed from this relaxed POPC. The 32-POPC bilayer was used to construct POPC/18.75%CHOL and POPC/18.75%DAG bilayer subunits. Three Cholesterol molecules and three DAGs were inserted as a group to create POPC/18.75%CHOL and POPC/18.75%DAG bilayer subunits, respectively. To construct the POPC/DAG/CHOL bilayer subunit, we used the 64-POPC bilayer and inserted cholesterols and DAGs together in two groups (i.e., 1DAG+2cholesterol and 2DAG+1cholesterol). The VMD program (http://www.ks.uiuc.edu/Research/vmd/) was then used to remove any bad links or overlaps that could happen after the cholesterol and DAG insertion.[36] Following this, the GROMACS[37] utility “genconf” was employed to replicate the systems of 32 and 64 to generate a new starting configuration consisting of 512 lipids for POPC/18.75%CHOL, POPC/18.75%DAG, and POPC/DAG/CHOL. All initial structures went through energy minimization using both the steepest descent and the conjugate gradient algorithms; each ran for 1000 steps to eliminate any bad contacts.

Acyl Chain Order Parameter

The order parameter was calculated differently at the double bond locations (i.e., carbon number 8 and 9 in Fig. 4b) from the previous simulations.[9,38,39] Current g_order tool in GROMACS (version 4.0.7) calculates the order parameter of an alkene carbon using the same equation for a methylene carbon, which is incorrect. We modified g_order tool, and used $-S_{CD}^{Sat}=\frac{2}{3}S_{xx}+\frac{1}{3}S_{yy}$ for saturated chain and $-S_{CD}^{Unsat}=\frac{1}{4}S_{zz}+\frac{3}{4}S_{yy}\mp\frac{\sqrt{3}}{2}S_{yz}$ for unsaturated chain, where S_{xx}, S_{yy}, S_{zz}, and S_{yz} are the order parameter tensors for angles between molecular axis and the bilayer normal calculated using the equation:

$$S_{ij}=\frac{1}{2}<3\cos(\theta_i)\cos\left(\theta_j\right)-\delta_{ij}>.$$

This modification is similar to g_order_new331 tool that was previously modified by Dr. Samuli Ollila.[40]

RESULTS AND DISCUSSION

Initial and Final Snapshots

Figure 2 depicts the initial and final snapshots of the top leaflets of the POPC/18.75%CHOL, POPC/18.75%DAG, and POPC/DAG/CHOL systems. For clarity, cholesterol and DAG are represented by the space-filling models, POPCs are represented by thin lines, and water molecules are not shown. In the initial configurations of POPC/18.75%CHOL and POPC/18.75%DAG (Figs. 2a & 2c), cholesterols and DAGs were arranged in 16 clusters and each cluster contained three molecules. The clusters in the initial POPC/DAG/CHOL system (Fig. 2e) were either 1CHOL+2DAG or 2CHOL+1DAG. After 500 ns simulation, the original artificially arranged clusters of cholesterol have dispersed, primarily into monomers (Fig. 2b). In comparison, DAGs have a less tendency to disperse as monomers; some DAGs are in small clusters (Fig. 2d). As shown in previous studies, cholesterol has a strong tendency be a monomer in a lipid bilayer, because the free energy cost of covering a cholesterol cluster by neighboring PC headgroups increases rapidly with the size of cluster.[11,19] An important feature in Fig. 2d is that some DAGs appear to extend their acyl chains laterally into the surrounding chain matrix (i.e., lateral extension). A visual inspection of 3D snapshots shows that the separation between two acyl chains is quite large for some DAGs. In order to judge whether it is statistically meaningful, we calculated the average distance between two acyl chains of POPC and compared it with that of DAG. The distance between C42 carbon of *sn*-1 chain and C24 carbon of *sn*-2 chain was used to represent the distance between two POPC chains; and the distance between C33 carbon of *sn*-1 chain and C15 carbon of *sn*-2 chain was used to represent the distance between two DAG chains (see Fig. 1a). As shown in Table 1, in every case, the average distance between two acyl chains of DAG is larger than that of POPC. Thus, DAG molecules have a statistical tendency to spread their chains. We believe that this type of chain conformation is resulted from the molecular shape of DAG. Although DAGs also have small hydrophilic headgroups and large hydrophobic bodies, they do not solely rely on the coverage from neighboring PC headgroups to avoid the unfavorable exposure to water: DAG can also insert their acyl chains into surrounding, as illustrated in Fig. 1c. Figure 2f is the final snapshot of the POPC/DAG/CHOL system. Interestingly, the lateral extension of DAG acyl chains near cholesterol molecules is suppressed by the presence of bulky sterol rings of cholesterol. As a consequence, DAGs become more relying on the umbrella coverage from PC headgroups in a lipid bilayer containing cholesterol.

Area per Lipid, Bilayer Thickness, and Volume per Lipid

The area per lipid ($A_{pl} = 2A_{box}/N_{lipid}$), volume per lipid ($V_{pl} = (V_{box} - N_{water}v_{water})/N_{lipid}$), and bilayer thickness ($h = V_{pl}/A_{pl}$) were calculated by averaging over the last 100 ns of the simulations, and the results are listed in Table 2. A_{pl} for pure POPC bilayer is 0.653 nm^2, which agrees reasonably well with the experimental values [0.63-0.68 nm[41,42]] and previous simulations results [0.65-0.67 nm^2, [18,39]]. For the POPC/18.75%CHOL bilayer, the area per lipid is 0.503 nm^2, which is close to the experimental value of 0.53 nm^2 [42] and the simulated value of 0.516 nm^2 by Pandit et al.[18] for POPC with 20% of cholesterol. Figure 3 shows A_{pl} for POPC/DAG bilayers as a function of DAG mole fraction. Since the cross-sectional area of DAG is less than that of POPC, as expected, A_{pl} shows a *monotonic* decrease as a function of DAG mole fraction. At the same DAG or cholesterol mole fraction (18.75%), the area per lipid of POPC/DAG system is larger than that of the POPC/18.75%CHOL system. On the other hand, the bilayer thickness of POPC/18.75%DAG system is smaller than that of POPC/18.75%CHOL system. Table 2 clearly shows that DAG decreases area per lipid and volume per lipid and increases bilayer thickness, which is similar to cholesterol in DOPC bilayers [9]. This behavior is expected, since DAG and cholesterol both are small-headgroup molecules.

Partial-Specific Areas

Figure 3 also shows the partial-specific areas of POPC and DAG in POPC/DAG bilayers, calculated using the method of Edholm and Nagle.[13] The partial specific area of DAG, $a_{DAG}(x)$ stays within a range of low value, between 0 and 0.1 nm^2. Since the measured area for a lipid with two tightly packed saturated chains is about 0.42 nm^2,[43] one would expect that a DAG molecule occupies at least 0.42 nm^2 lateral area in a fluid-phase PC bilayer. By definition, $a_{DAG}(x)$ is the increase of total bilayer area at the bilayer composition x by adding one more DAG molecule to the bilayer, while keeping all other parameters constant. Thus, the low partial-specific area of DAG indicates a far less than expected increase of total bilayer area by adding a DAG to a POPC bilayer. This result clearly shows that DAG produces the "condensing effect" in POPC bilayers. Previously, other researchers have found that cholesterol has a negative partial-specific area in DOPC and POPC lipid bilayers at low cholesterol mole fractions, and the value becomes positive above cholesterol mole fraction of 0.1.[9,13,18] Thus, comparing to DAG, cholesterol produces a stronger condensing effect. On the other hand, the partial specific area of POPC, $a_{POPC}(x)$, stays at a narrow range, from 0.653 to 0.638 nm^2. This shows that the condensing effect is mainly produced by DAG, not by POPC. What causes the condensing effect in lipid bilayers? We have suggested that the condensing effect is a consequence of the umbrella interaction between cholesterol and PC.[20,44] A recent coarse-grained simulation by de Meyer and Smit demonstrated that the condensing effect is indeed directly resulted from the mismatch between cholesterol small polar head and its large nonpolar body.[12] Pandit et al. showed that ceramide, another lipid molecule with a small polar head, also induces condensing effect in POPC bilayers.[18] Our result further supports the conclusion.

Acyl Chain Order Parameter

Figure 4 shows the order parameters of POPC and DAG chains at each carbon atom position. It has been well established that the higher the cholesterol mole fraction, the higher the order parameter.[9,45] We modified g_order tool in GROMACS (see SIMULATION METHOD), and our order parameters for pure POPC are very close to the experimental results[46] and some previous simulation results[18,40,47]. The order parameter for POPC with 18.75 % of cholesterol is also close to the previous simulation result for POPC with 20 % of cholesterol.[18] The acyl chains of POPC have the highest order in the POPC/18.75%CHOL system. The *cis* double bond in *sn-2* chain of POPC produces a sharp local drop of chain order parameter. Similarly, the order parameter of acyl chains of DAG increases with DAG concentration as shown in Fig. 4c and 4d. Since the order parameter of DAG chains is higher in POPC/DAG/CHOL system (with 9.3755% of DAG and 9.375% of cholesterol) than that in POPC/12.5%DAG system, it indicates that cholesterol also increases the order parameter of DAG chains. A general picture emerges from Figure 4 that the addition of cholesterol, or DAG, or both can all increase the order of chains. At the same concentration, cholesterol is slightly more effective than DAG in ordering POPC acyl chains.

Cholesterol Tilt Angle

The cholesterol tilt angle is defined as the angle between the vector connecting C21 and C5 atoms of cholesterol (see Figure 1a) and the bilayer normal. It is well known that cholesterol tile angle decreases and the order of a bilayer increases as cholesterol concentration increases.[9,14,15,17] Using solid-state NMR, the cholesterol tilt angle in DPPC bilayer containing 30% cholesterol at 47 °C was determined to be 18.1° by Guo et al.[48] The cholesterol tilt angle in DPPC bilayer containing 20% cholesterol at 50 °C was found to be 19.8° in a number of MD simulation studies.[49-51] The tilt angle is larger in DOPC bilayers: Previous MD simulations showed that the cholesterol tile angle in DOPC bilayer containing 20% cholesterol at 50 °C is about 23.5°-24.7°.[9,49] Figure 5 shows the probability distributions of cholesterol tilt angle for POPC/18.75%CHOL and POPC/DAG/CHOL

systems. The average cholesterol tilt angle in POPC/18.75%CHOL system is 21.7±1.5°, which is in line with other studies. Interestingly, the average cholesterol tilt angle in the POPC/DAG/CHOL system (21.6±2.2°) is very similar to that in the POPC/18.75%CHOL system. Since the POPC/DAG/CHOL system contained 9.375% of cholesterol and 9.375% of DAG (Table 2), our data shows that DAG also decreases cholesterol tilt angle; otherwise, one would expect a larger cholesterol tilt angle in POPC/DAG/CHOL system.

Electron Density

Figure 6 shows the electron density profiles of POPC, cholesterol, DAG and water across the lipid bilayers in four systems. For the electron density profiles of POPC (Fig. 6a), the addition of cholesterol, or DAG, or both, produces two noticeable effects: (i) The profiles expand in the direction of bilayer normal, indicating an increase of bilayer thickness; (ii) the peaks, that largely correspond to the distribution of POPC headgroups [9], become sharper, indicating that POPC headgroups become more parallel to the bilayer-aqueous interfaces. The effects are largest in the POPC/18.75%CHOL system and smallest in the POPC/18.75%DAG system, closely correlated to the order of acyl chains (Fig. 4). The electron density profile of DAG in the POPC/DAG/CHOL system is also very similar to that in the POPC/18.75%DAG system (Fig. 6c).

The relative positions of POPC, DAG, and CHOL in the bilayers are illustrated in Figure 7. In the POPC/18.75%CHOL system, on average, O6 atom of cholesterol is located ~2.0 Å below the C13 atom of POPC. The C4 atom of DAG is located ~1.9 Å below the C13 atom of POPC in the POPC/18.75%DAG system. Our result is consistent with Schorn and Marsh's experimental finding that DAGs are situated approximately two CH_2 groups deeper in the hydrophobic interior.[5] Finally, in the POPC/DAG/CHOL system, O6 atom of cholesterol and C4 atom of DAG are located about 1.4 Å and 2.4 Å below the C13 atom of POPC, respectively. These relative positions are consistent with our interpretation that headgroups of POPC provide the umbrella coverage for both cholesterol and DAG (Fig. 1b and 1c).

The Umbrella Effect

Figure 8a quantifies the Umbrella effect on cholesterol in the POPC/18.75%CHOL bilayer. Two 2D radial distribution function (RDF) were calculated in the plane parallel to the bilayer surface: one between the O6 atom of cholesterol and the N4 atom of PC's choline group, and a second between cholesterol O6 and PC's phosphate residue P8, represented by the two white dashed lines in Fig. 1b. Similar to a previously study [11], the RDF of $O6_{CHOL}$-$N4_{POPC}$ is higher than the RDF of $O6_{CHOL}$-$P8_{POPC}$ for the distance less than ~0.4 nm from a cholesterol, and the relation is reversed for the distance between ~0.4 and ~0.8 nm, which indicates that the first layer of PC headgroups next a cholesterol molecule (≤ 0.8 nm) has a statistical tendency to extend their P-N vectors toward the cholesterol in order to cover cholesterol's hydrophobic body, as illustrated in Fig. 1b. The two RDFs cross over several more times between 0.8 and 3 nm, indicating that the orientation order of PC head groups extends up to about three molecules away from a cholesterol molecule. An important new result in this study is that POPC headgroups also provide the umbrella coverage for DAGs: In the POPC/18.75%DAG system, the RDF of $O2_{DAG}$- $N4_{POPC}$ is higher than the RDF of $O2_{DAG}$- $P8_{POPC}$ for the distance less than 0.25 nm from a DAG, and the relation is also reversed for the distance between 0.25 and 0.65 nm (Fig. 8b). It appears that the first layer of POPC headgroups next to a DAG hydroxyl group is about 1.5 Å closer than that next to a cholesterol hydroxyl group. This is understandable, since a DAG does not have the bulky sterol rings of cholesterol to prevent surrounding PCs getting closer. In addition, the second layer of PC headgroups, located roughly between 0.7 to 1.7 nm from a DAG, is also ordered with their P-N vectors preferentially pointing to the DAG, likely due to the dipole-dipole

interaction with the headgroups of PC in the first layer. To facilitate the discussion, we define a numerical parameter, named the "Umbrella Index" (*UI*), to quantitatively describe the orientational order of phospholipid headgroups surrounding a cholesterol molecule or a DAG. For cholesterol, *UI* is defined as $UI \equiv \int |\mathrm{RDF}(\mathrm{O6}_{\mathrm{CHOL}}\text{-}\mathrm{N4}_{\mathrm{PC}}) - \mathrm{RDF}(\mathrm{O6}_{\mathrm{CHOL}}\text{-}\mathrm{P8}_{\mathrm{PC}})|\, dx$ for x from 0 to 3 nm. Visually, *UI* is the total area between the two RDF from 0 to 3 nm in Figure 8. A larger *UI* value would indicate a higher orientational order of PC headgroups. The calculated *UI* is 0.206 for cholesterol in the POPC/18.75%CHOL system and 0.239 for DAG in the POPC/18.75%DAG system, suggesting that a DAG receives more PC headgroup coverage than a cholesterol molecule, at the same concentration. The difference is likely resulted from the smaller headgroup/body areal ratio of DAG. Both DAG and cholesterol have hydroxyl as their hydrophilic head. Although DAG is in a fluid-phase in POPC bilayer, the lower limit of its cross-sectional area in its hydrophobic acyl-chain region, 42 $Å^2$, can be estimated from a gel-phase lipid bilayer[43]. On the other hand, the estimation of the cross-sectional area of cholesterol's sterol rings is ranging 32-38 $Å^2$.[9] Thus, it is reasonable that DAG needs more umbrella coverage from POPC headgroups.

We have shown that our simulation data is consistent with the umbrella model; however, we did not compare our results with the Condensed-Complex model.[52,53] The primary reason is that the model does not have a specific prediction for the physical structure of the hypothesized lipid-cholesterol stoichiometric complex. In addition, it becomes increasingly clear that the condensing effect can be induced by a number of membrane molecules, including cholesterol, DAG, ceramide,[18] and other sterols,[17,54] although their effectivenesses may vary. These molecules have different chemical structures but share a common molecular shape: a small hydrophilic headgroup and a large hydrophobic body. Thus, these results strongly indicate that the condensing effect is more associated with the shape of molecule than stoichiometric complex.

Figures 8c and 8d illustrate the umbrella coverage for DAG and cholesterol in the POPC/DAG/cholesterol ternary mixture. Interestingly, in the POPC/DAG/cholesterol ternary system (Fig. 8d), the calculated *UI* for DAG becomes significantly larger (*UI* = 0.285) than that in the POPC/18.75%DAG system (*UI* = 0.239). In the ternary system, the lateral extension of DAG acyl chains is visibly suppressed by the bulky rigid sterol rings of cholesterol (Fig. 2f), and DAGs become more relying on the umbrella coverage from PC headgroups. For cholesterol, the umbrella index also increases from 0.206 to 0.244. This indicates that the PC headgroups become highly ordered in POPC/DAG/cholesterol ternary system. A visual inspection of simulation snapshots confirmed that DAG received more headgroup coverage from POPC than cholesterol does in POPC/DAG/cholesterol ternary system.

The increase of spacing between PC headgroups

One of the important effects of incorporating DAG into a lipid bilayer is the increase of spacing between phospholipid headgroups. It has been long suggested that the increase of spacing is crucial for the binding of protein kinase C to lipid membranes or the activation of phospholipases.[1,3,55] Statistically, we found that DAGs indeed increase the average distance between PC headgroups. Figure 9 shows the 2D RDFs between O11 atoms of POPC in various bilayers. At the short distance, the RDF is the lowest in POPC bilayer containing 18.75% of DAG, which indicates that DAG is more effect than cholesterol in increasing the spacing between PC headgroups, directly correlated with the smaller headgroup/body ratio of DAG. Interestingly, the conventional wisdom has been that a DAG with a small polar headgroup can wedge into a phospholipid bilayer and create an opening direct above the DAG molecule, as illustrated in Fig. 10a;[1,3,55] however, our simulations show that this may not be correct. Fig. 10c is a top-view snapshot of POPC bilayer containing 6.25% of DAG. The white arrows represent the P-N vectors of POPC headgroups, and DAG molecules are

represented by the space-filling model. A careful examination of Fig. 10c shows that in almost every case, there are P-N vectors of POPC distributed above a DAG headgroup, and this coverage of DAG by POPC headgroups is driven by the umbrella effect discussed earlier. Fig. 10c also shows that large headgroup spacing usually occurs between the first and the second nearest-neighbor PCs from a DAG. This observation also explains why the distance distribution of the second-nearest neighbor PCs from a DAG is wider than the size of a PC molecule (i.e., from 0.7 to 1.7 nm in Fig. 8b). Fig. 10b is a schema that illustrates the distribution of spacing between PC headgroups near a DAG molecule. In order to confirm the conceptual picture shown in Fig. 10b, we analyzed the distributions of POPC headgroups and acyl chains around DAG in POPC/6.25%DAG system as well as around POPC in pure POPC bilayer. To calculate RDFs, the position of a POPC headgroup was simply taken as the midpoint of its P-N vector, and the center of mass of two acyl chains from the same POPC was used to represent the position of POPC chains. As shown in Fig. 11, in POPC/6.25%DAG system, the distribution of PC headgroups (i.e., P-N vectors) around DAG O2 oxygen has a large peak at ~0.29 nm and a small peak at ~0.48 nm. Judging from the distance, these two peaks correspond to the nearest-neighbor POPC headgroups providing the umbrella coverage to DAGs. Two close peaks suggest that certain orientations of PC headgroup may be preferred. At the same distance range, the RDF of POPC acyl chains is significantly lower than the RDF of POPC headgroups, which clearly indicates that the POPC headgroups next to a DAG tilt towards the DAG. Furthermore, from the distance of 0.6 nm to 1.4 nm, the RDF of POPC headgroup is lower than the RDF of POPC chains and has a minimum at ~0.75 nm, which shows that there are more chains than headgroups in this region. Thus, the spacing between PC headgroups in this region is larger compared to random distribution. For distances larger than 1.4 nm, two RDFs become similar, and the spacing between POPC headgroup returns normal. This result is consistent with the conceptual picture in Fig. 10b. In contrast, the distribution of POPC headgroups around a POPC has totally different behavior: the chance of other POPC headgroups positioned within 0.45 nm from a POPC headgroup is very low.

Lateral Diffusion of Lipids

The mean square displacements (MSD or $<r(t)^2>$) of POPC, cholesterol, and DAG as functions of time are plotted in Fig. 12. The systems were allowed to relax for the first 100ns, and the calculations were performed for the remaining time. All curves have three distinct sections: an initial rapid rise, a linear portion, and a noisy section at end. The initial rapid rise (100-105 ns) of MSD is primarily due to the local motions of molecules, the linear portion reflects the true lateral diffusion behavior, and the noisy section at end is due to poor statistics for large displacements. The 2D lateral diffusion coefficient, $D = ¼d<r(t)^2>/dt$, was obtained by fitting the linear portion of MSD curves, using the least squares method. For pure POPC, POPC/18.75%CHOL, POPC/DAG/CHOL, and POPC/18.75%DAG systems, The MSD curves were calculated for the time periods of 100-500ns and 150-500ns, and D was calculated using the average of the linear fit of 120-170ns and 170-220ns sections of the MSD curves. Table 3 lists the calculated lateral diffusion coefficients. The calculated D of POPC in pure POPC bilayer is 11.44×10^{-8} cm^2/s, which is close to experimental results [$8\text{-}10\times10^{-8}$ cm^2/s].[56-58] In the POPC/18.75%CHOL system, cholesterol slows down the diffusion of POPC, and D decreases to 4.41×10^{-8} cm^2/s, which is close to the experimental value of 3.21×10^{-8} cm^2/s by ESR.[56] On the other hand, the diffusion coefficient of POPC is 8.34×10^{-8} cm^2/s in POPC/18.75%DAG system. Thus, DAG also reduces the diffusion of POPC, but not as much as cholesterol. The most interesting result is that the lowest diffusion coefficients for POPC, DAG and cholesterol are all found in the POPC/DAG/CHOL system, which suggests that cholesterol and DAG at 1:1 ratio is more effective than cholesterol or DAG alone in slowing down diffusion.

CONCLUSIONS

In this comparative study, we found that DAG produces some very similar effects to PC bilayers as cholesterol: increasing acyl chain order and bilayer thickness, reducing lateral diffusion of molecules, and producing the well-known “condensing effect”. This similarity in functionality is resulted from their similarity in molecular shape: small hydrophilic heads and large hydrophobic bodies. In a lipid bilayer, cholesterol mainly relies on the coverage of neighboring phospholipid headgroups to avoid the unfavorable exposure of hydrophobic part to water, however DAG uses the combination of PC headgroup coverage and the lateral extension of its acyl chains. At the same concentration, cholesterol is more effective than DAG in producing the above effects, probably due to its rigid sterol rings. In a lipid bilayer, DAG receives more coverage from POPC headgroups than cholesterol does, likely due to its smaller headgroup/body areal ratio. Thus, DAG can strongly modulate the physical state and chemical activity of lipid in membranes. Our results provide explanations to the previous finding that cholesterol can amplify DAG activities [21]. DAGs are also found to be able to increase the average distance between PC headgroups, but the conventional wisdom that the spacing created by a DAG is directly above the DAG molecule turns out to be incorrect. We found that the largest spacing usually occurs between the first and the second nearest-neighbor PC headgroups from a DAG, which could have a significant implication for activating protein kinase C and other enzymes by DAGs.

Supplementary Material

Refer to Web version on PubMed Central for supplementary material.

Acknowledgments

This work was supported by the NIH grant R01 GM077198-01A1 subaward 49238-8402. The authors acknowledge the High Performance Computing Center (HPCC) at Texas Tech University for providing HPC resources for this work. The authors thank Dr. Frederick A. Heberle and David Ackerman for pointing out the problem with g_order tool in GROMACS, and Dr. Ramon Reigada for sending us g_order_new331 tool.

References

1. Gomez-Fernandez JC, Corbalan-Garcia S. Chem Phys Lipids. 2007; 148:1. [PubMed: 17560968]
2. Takai YK, Kikkawa A, Mori U, Nishizuka Y. Biochem. Biophys. Res. Commun. 1979; 91:1218. [PubMed: 526298]
3. Das S, Rand RP. Biochemistry. 1986; 25:2882. [PubMed: 3718927]
4. Goldberg EM, Lester DS, Borchardt DB, Zidovetzki R. Biophys J. 1994; 66:382. [PubMed: 8161692]
5. Schorn K, Marsh D. Biochemistry. 1996; 35:3831. [PubMed: 8620006]
6. Demel RA, van Deenen LLM, Pethica BA. Biochim Biophys Acta. 1967; 135:11.
7. Leathes JB. Lancet. 1925; 208:853.
8. Stockton BW, Smith ICP. Chem Phys Lipids. 1976:17.
9. Alwarawrah M, Dai J, Huang J. J Phys Chem B. 2010; 114:7516. [PubMed: 20469902]
10. Berkowitz ML. Biochim Biophys Acta. 2009; 1788:86. [PubMed: 18930019]
11. Dai J, Alwarawrah M, Huang J. J Phys Chem B. 2010; 114:840. [PubMed: 20041657]
12. de Meyer F, Smit B. Proc Natl Acad Sci U S A. 2009; 106:3654. [PubMed: 19225105]
13. Edholm O, Nagle JF. Biophysical Journal. 2005; 89:1827. [PubMed: 15994905]
14. Hofsäß C, Lindahl E, Edholm O. Biophysical Journal. 2003; 84:2192. [PubMed: 12668428]
15. Niemela PS, Hyvonen MT, Vattulainen I. Biochim Biophys Acta. 2009; 1788:122. [PubMed: 18817748]

16. Pitman MC, Suits F, Mackerell AD Jr. Feller SE. Biochemistry. 2004; 43:15318. [PubMed: 15581344]
17. Rog T, Pasenkiewicz-Gierula M, Vattulainen I, Karttunen M. Biochim Biophys Acta. 2009; 1788:97. [PubMed: 18823938]
18. Pandit SA, Chiu SW, Jakobsson E, Grama A, Scott HL. Biophys J. 2007; 92:920. [PubMed: 17071659]
19. Huang J. Methods Enzymol. 2009; 455:329. [PubMed: 19289212]
20. Huang J, Feigenson GW. Biophys J. 1999; 76:2142. [PubMed: 10096908]
21. Armstrong D, Zidovetzki R. Biophys J. 2008; 94:4700. [PubMed: 18326666]
22. Berger O, Edholm O, Jahnig F. Biophys J. 1997; 72:2002. [PubMed: 9129804]
23. Holtje M, Forster T, Brandt B, Engels T, von Rybinski W, Holtje HD. Biochim Biophys Acta. 2001; 1511:156. [PubMed: 11248214]
24. van Gunsteren, WF.; Kruger, P.; Billeter, SR.; Mark, AE.; Eising, AA.; Scott, WRP.; Huneberg, PH.; Tironi, IG. Biomos Hochschulverlag AG an der ETH Zurich. Groningen; Germany: 1996.
25. Becke AD. Journal of Chemical Physics. 1993; 98:5648.
26. Lee CT, Yang WT, Parr RG. Phys Rev B. 1988; 37:785.
27. Stephens PJ, Devlin FJ, Chabalowski CF, Frisch MJ. Journal of Physical Chemistry. 1994; 98:11623.
28. Vosko SH, Wilk L, Nusair M. Canadian Journal of Physics. 1980; 58:1200.
29. Dill JD, Pople JA. J. Chem. Phys. 1975; 62:2921.
30. Francl MM, Pietro WJ, Hehre WJ, Binkley JS, Gordon MS, Defrees DJ, Pople JA. Journal of Chemical Physics. 1982; 77:3654.
31. Hehre WJ, Ditchfield R, Pople JA. J. Chem. Phys. 1972; 56:2257.
32. Hoover WG. Phys Rev A. 1985; 31:1695. [PubMed: 9895674]
33. Parinello M, Rahman A. J. Appl. Phys. 1981; 52:7182.
34. Essmann U, Perera L, Berkowitz ML, Darden T, Lee H, Pedersen LG. Journal of Chemical Physics. 1995; 103:8577.
35. Schuettelkopf AW, van Aalten DMF. Acta Crystallographica. 2004; D60:1355.
36. Humphrey W, Dalke A, Schulten K. J Mol Graph. 1996; 14:33. [PubMed: 8744570]
37. Van Der Spoel D, Lindahl E, Hess B, Groenhof G, Mark AE, Berendsen HJ. J Comput Chem. 2005; 26:1701. [PubMed: 16211538]
38. Mukhopadhyay P, Monticelli L, Tieleman DP. Biophys J. 2004; 86:1601. [PubMed: 14990486]
39. Zhang Z, Bhide SY, Berkowitz ML. J Phys Chem B. 2007; 111:12888. [PubMed: 17941659]
40. Ollila S, Hyvonen MT, Vattulainen I. J Phys Chem B. 2007; 111:3139. [PubMed: 17388448]
41. Kucerka N, Tristram-Nagle S, Nagle JF. J Membr Biol. 2005; 208:193. [PubMed: 16604469]
42. Smaby JM, Momsen MM, Brockman HL, Brown RE. Biophys J. 1997; 73:1492. [PubMed: 9284316]
43. Scheffer L, Solomonov I, Weygand MJ, Kjaer K, Leiserowitz L, Addadi L. Biophys J. 2005; 88:3381. [PubMed: 15722431]
44. Parker A, Miles K, Cheng KH, Huang J. Biophys J. 2004; 86:1532. [PubMed: 14990480]
45. Huber T, Rajamoorthi K, Kurze VF, Beyer K, Brown MF. J Am Chem Soc. 2002; 124:298. [PubMed: 11782182]
46. Seelig J, Waespe-Sarcevic N. Biochemistry. 1978; 17:3310. [PubMed: 687586]
47. Aittoniemi J, Niemela PS, Hyvonen MT, Karttunen M, Vattulainen I. Biophys J. 2007; 92:1125. [PubMed: 17114220]
48. Guo W, Kurze V, Huber T, Afdhal NH, Beyer K, Hamilton JA. Biophysical Journal. 2002; 83:1465. [PubMed: 12202372]
49. Aittoniemi J, Rog T, Niemela P, Pasenkiewicz-Gierula M, Karttunen M, Vattulainen I. Journal of Physical Chemistry B. 2006; 110:25562.
50. Rog T, Pasenkiewicz-Gierula M, Vattulainen I, Karttunen M. Biophysical Journal. 2007; 92:3346. [PubMed: 17293396]

51. Vainio S, Jansen M, Koivusalo M, Rog T, Karttunen M, Vattulainen I, Ikonen E. Journal of Biological Chemistry. 2006; 281:348. [PubMed: 16249181]
52. Radhakrishnan A, McConnell H. Proc Natl Acad Sci U S A. 2005; 102:12662. [PubMed: 16120676]
53. Radhakrishnan A, McConnell HM. Biochemistry. 2000; 39:8119. [PubMed: 10889017]
54. Su YL, Li QZ, Chen L, Yu ZW. Colloid Surf. A-Physicochem. Eng. Asp. 2007; 293:123.
55. Bell RM, Burns DJ. J Biol Chem. 1991; 266:4661. [PubMed: 2002013]
56. Shin YK, Freed JH. Biophys J. 1989; 55:537. [PubMed: 2539210]
57. Kuo AL, Wade CG. Biochemistry. 1979; 18:2300. [PubMed: 444458]
58. Gaede HC, Gawrisch K. Biophys J. 2003; 85:1734. [PubMed: 12944288]

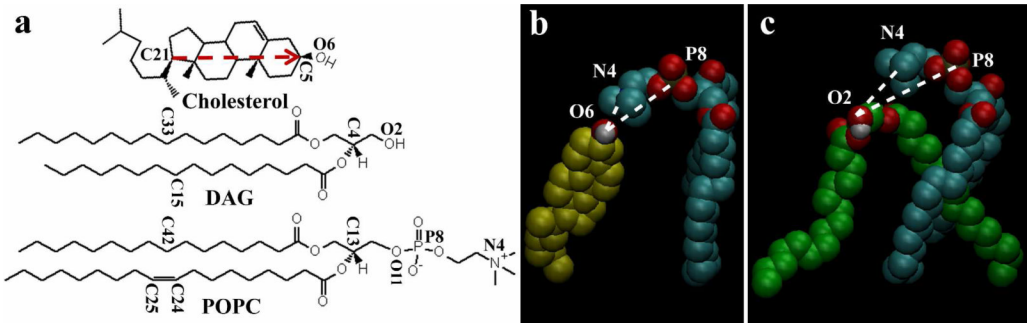

Figure 1.

(a) Chemical structures of cholesterol, di16:0DAG, and POPC. The vector connecting C21 and C5 atoms of cholesterol (red arrow) represents the orientation of a cholesterol molecule. Atom indices, such as C4 and O2 of DAG, are the atom indices names in the corresponding molecules structure PDB files. (b) Illustration of a headgroup of PC orienting toward cholesterol (in yellow) to provide the umbrella coverage. The red spheres are oxygen atoms. (c) Illustration of the lateral insertion of DAG chains (in green) and the umbrella coverage by PC headgroup to DAG.

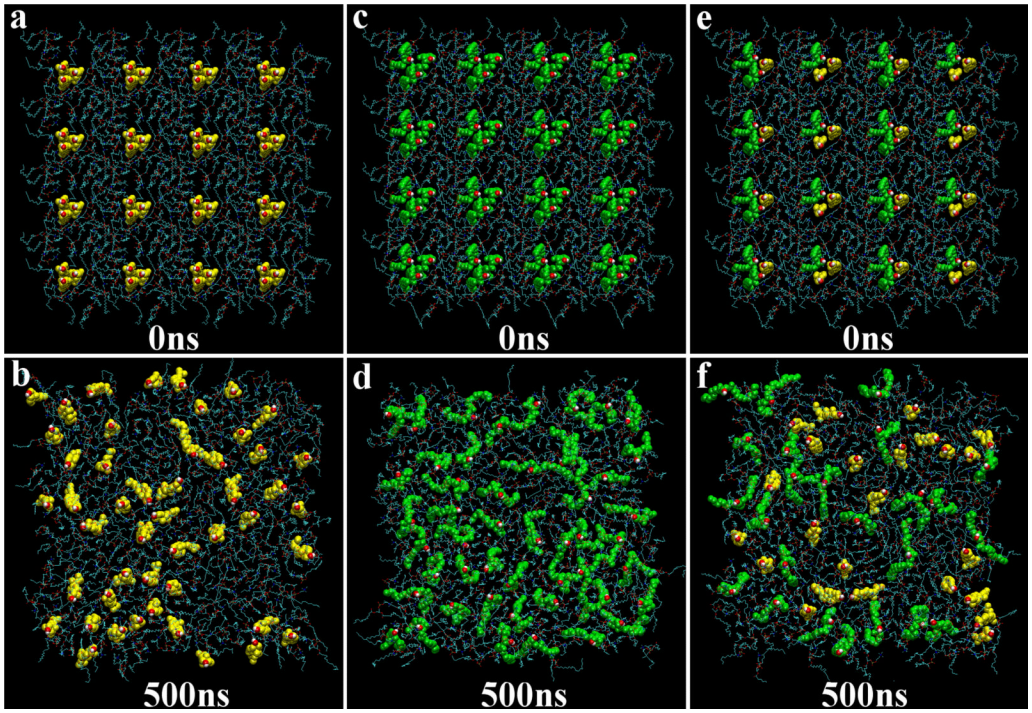

Figure 2.

(a) and (b): The initial and final snapshots of POPC/18.75%CHOL system. Only the lipids on the top leaflet are shown. POPCs are represented by thin lines, and cholesterol molecules (in yellow) are represented by the space-filling model. The red spheres are O6 atoms of cholesterol. (c) and (d): The initial and final snapshots of POPC/18.75%DAG system. DAGs (in green) are represented by the space-filling model. The red spheres are O2 atoms of DAG. (e) and (f): The initial and final snapshots of POPC/DAG/CHOL system.

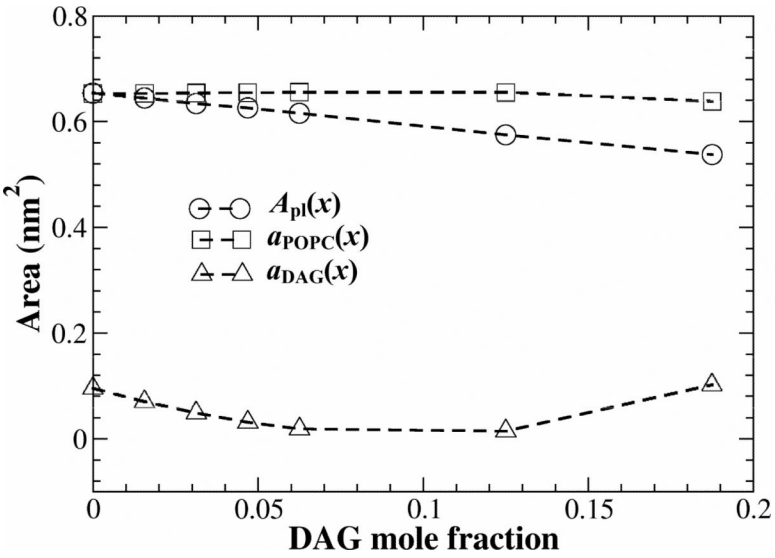

Figure 3.

Area per lipid ($A_{pl}(x)$), and partial-specific areas of POPC ($a_{POPC}(x)$) and DAG ($a_{DAG}(x)$) vs. DAG mole fraction in POPC/DAG bilayers.

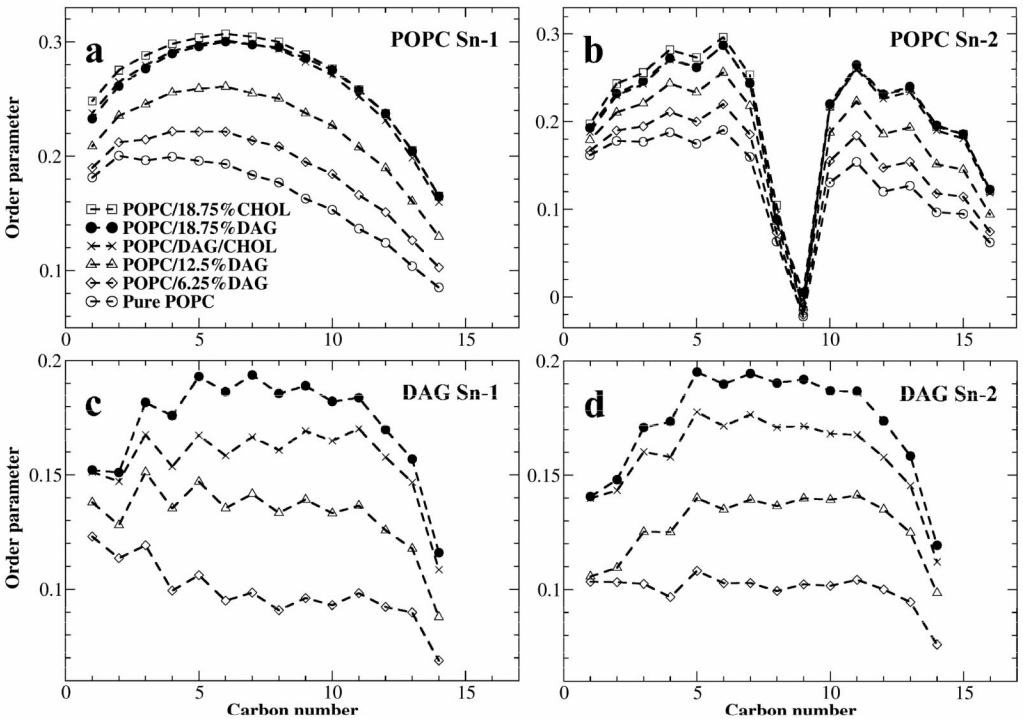

Figure 4.

(a) and (b): The order parameter of POPC acyl chains. (c) and (d): The order parameter of DAG acyl chains.

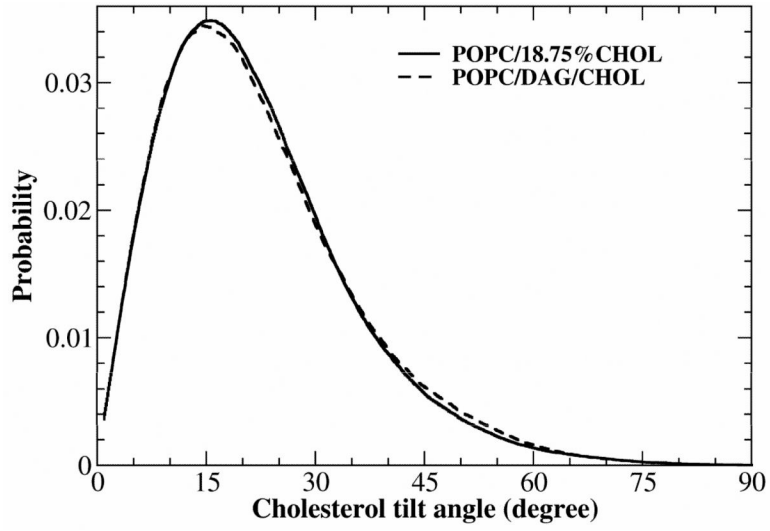

Figure 5.

Tilt angle distributions between the bilayer normal and the vector connecting C21 and C5 atoms of cholesterol in POPC/18.75%CHOL and POPC/DAG/CHOL bilayers systems.

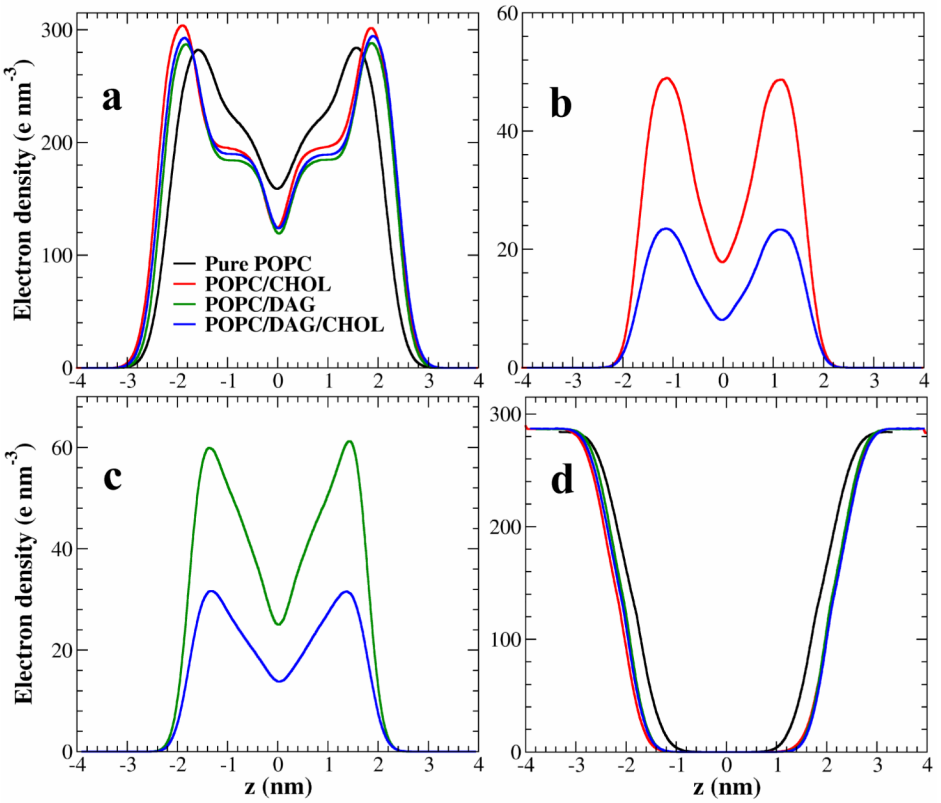

Figure 6.
The electron density profiles of POPC (a), cholesterol (b), DAG (c), and water (d) across the bilayer in various systems.

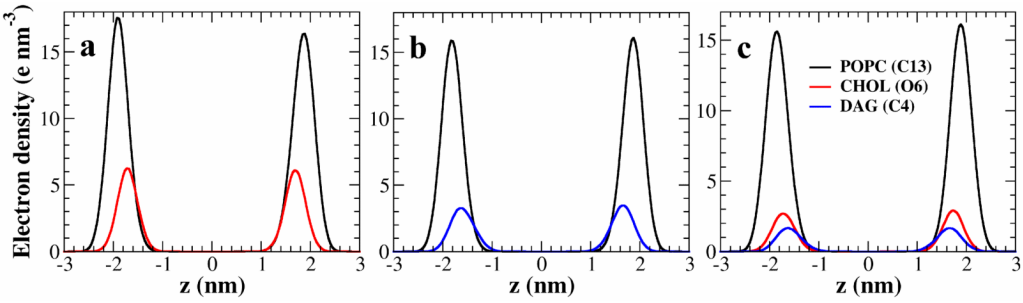

Figure 7.

The electron density profiles of C13 atom of POPC, O6 of cholesterol, and C4 of DAG, which illustrate the relative positions of these lipids in the lipid bilayers. (a) in POPC/18.75%CHOL; b) in POPC/18.75%DAG; and c) in POPC/DAG/CHOL system.

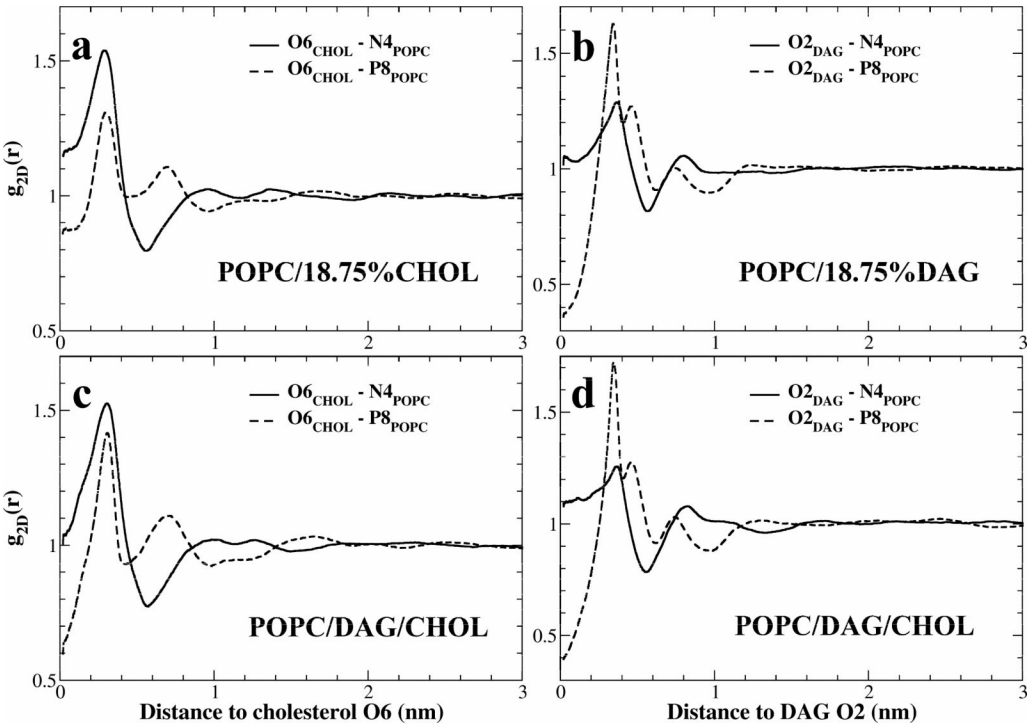

Figure 8.

The umbrella coverage on cholesterol or DAG by POPC headgroups quantified by radial distribution functions (RDF). (a) and (c): The RDFs between cholesterol oxygen O6 and POPC nitrogen N4 of choline group or phosphate P8. (b) and (d): RDFs between DAG oxygen O2 and POPC nitrogen N4 of choline group or phosphate P8.

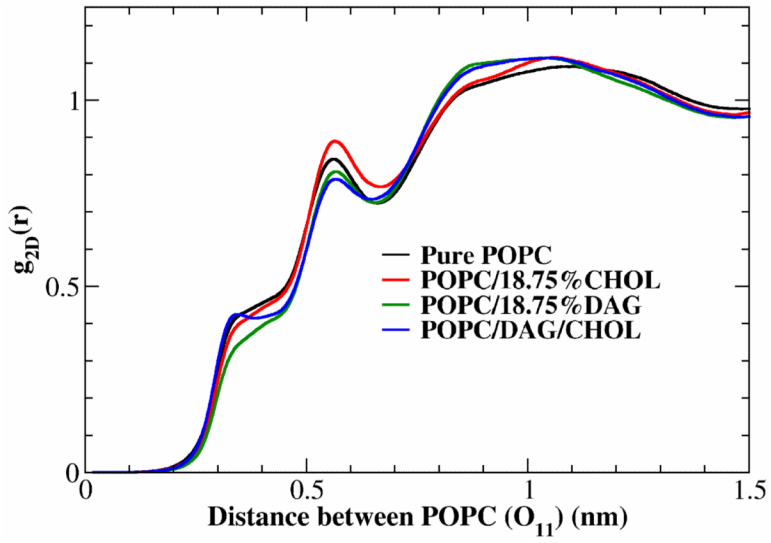

Figure 9.
2D RDF of O11 atom of POPC headgroup.

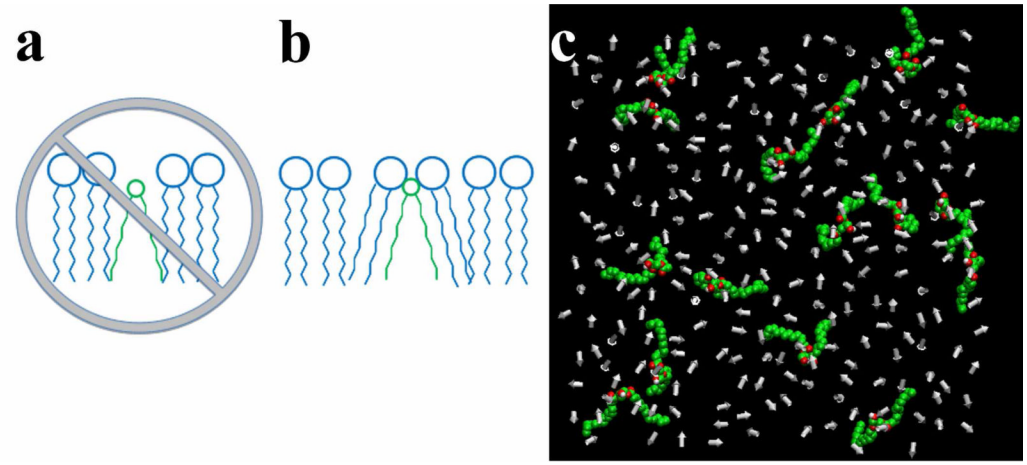

Figure 10.

(a) The conventional wisdom of the creating spacing between PC headgroups by a DAG in a lipid bilayer, which is found to be incorrect in this study. (b) Conceptual illustration of our simulation result that the largest space created by a DAG is usually between the 1st and the 2nd nearest-neighbor PC headgroups from a DAG. (c) A top-view snapshot of POPC bilayer contained 6.25% of DAG. DAGs are represented by the space-filling model, and the white arrows represent the P-N vectors of POPC headgroups.

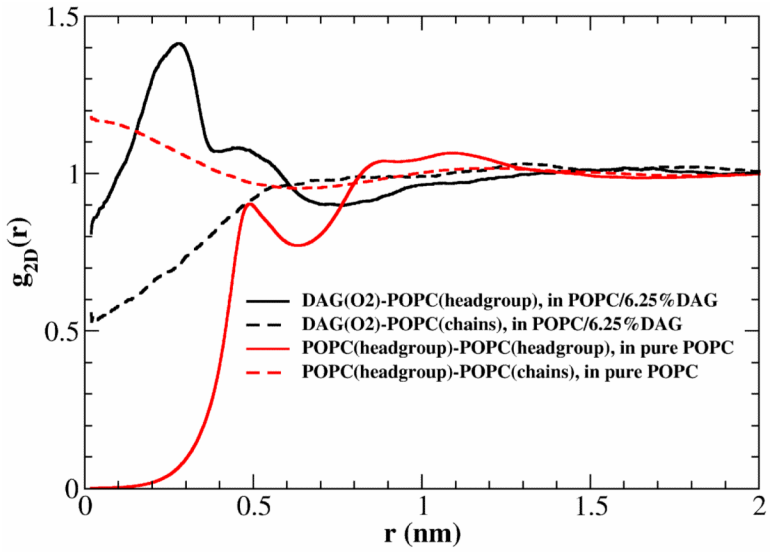

Figure 11.

2D RDFs illustrate the distributions of POPC headgroups and acyl chains around DAG in POPC/6.25%DAG system and around POPC in pure POPC bilayer. The position of a POPC headgroup was taken as the midpoint of its P-N vector, and the center of mass of two acyl chains from the same POPC was used to represent the position of POPC chains.

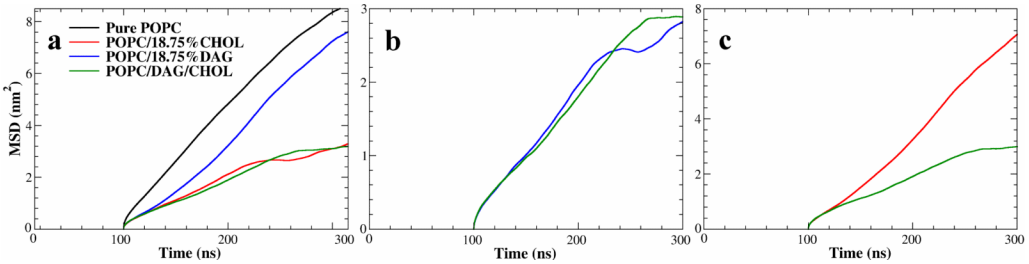

Figure 12.
The mean square distance of POPC (a), cholesterol (b), and DAG (c) vs. time. The calculations started at 100 ns.

Table 1

Average distances between two acyl chains of POPC or DAG.

Systems	CHOL%	DAG%	POPC (C24-C42) (nm)	DAG (C15-C33) (nm)
Pure POPC	0	0	1.12±0.02	-
POPC/18.75%CHOL	18.75	0	0.96±0.02	-
POPC/CHOL/DAG	9.375	9.375	0.98±0.02	1.10±0.04
POPC/DAG	0	18.75	0.99±0.02	1.06±0.03
	0	12.50	1.04±0.02	1.16±0.03
	0	6.25	1.09±0.02	1.22±0.06
	0	4.69	1.10±0.01	1.27±0.06
	0	3.13	1.10±0.02	1.24±0.09
	0	1.56	1.12±0.02	1.24±0.10

Table 2

Area per lipid (A_{pl}), bilayer height (h), and volume per lipid (V_{pl}) in various systems.

Systems	CHOL%	DAG%	A_{pl}(nm^2)	h (nm)	V_{pl}(nm^3)
Pure POPC	0	0	0.653±0.005	3.87±0.03	1.264±0.004
POPC/18.75%CHOL	18.75	0	0.503±0.004	4.44±0.04	1.116±0.004
POPC/CHOL/DAG	9.375	9.375	0.524±0.004	4.38±0.04	1.147±0.004
POPC/DAG	0	18.75	0.538±0.005	4.38±0.04	1.177±0.004
	0	12.50	0.575±0.006	4.19±0.04	1.206±0.004
	0	6.25	0.616±0.006	4.01±0.04	1.235±0.004
	0	4.69	0.626±0.006	3.97±0.04	1.242±0.004
	0	3.13	0.634±0.005	3.94±0.03	1.249±0.004
	0	1.56	0.644±0.006	3.90±0.04	1.256±0.004

J Chem Theory Comput. Author manuscript; available in PMC 2013 February 14.

Table 3

Lateral diffusion coefficient of POPC, cholesterol, DAG, and water (SOL).

	Lateral diffusion coefficient (10^{-8} cm^2/s)			
System	**POPC**	**CHOL**	**DAG**	**SOL**
Pure POPC	11.44±0.01	-	-	3119.45±0.04
POPC/18.75%CHOL	4.41±0.01	4.12±0.01	-	3590.98±0.23
POPC/18.75%DAG	8.34±0.01	-	8.11±0.01	3539.59±0.17
POPC/DAG/CHOL	4.16±0.01	4.11±0.01	3.90±0.01	3572.76±0.10